GEOMETRY EFFECT ON PHOTOVOLTAIC-THERMOELECTRIC TRANSIENT PERFORMANCE

Samson Shittu[1], Guqiang Li [1*], Xudong Zhao [1*], Xiaoli Ma [1]

[1] School of Engineering and Computer Science, University of Hull, HU6 7RX, UK.

Corresponding authors. E-mail: Guiqiang Li@hull.ac.uk (G.Li); Xudong.Zhao@hull.ac.uk (X.Zhao)

ABSTRACT

This paper presents a three-dimensional numerical investigation on the effect of thermoelectric geometry on hybrid photovoltaic-thermoelectric (PV-TE) performance under varying weather conditions. Four thermoelectric (TE) geometries corresponding to four different cases are considered under transient conditions and different thermoelectric leg height are investigated. The effect of the thermoelectric geometry and leg height on the efficiency and power output of the PV-TE is studied for a duration of 24 hours under actual weather conditions (solar radiation, ambient temperature and wind speed). Results show that the symmetrical thermoelectric legs (case 1) are beneficial for hybrid PV-TE under transient conditions. Although asymmetrical thermoelectric legs (case 4) provide higher thermoelectric generator (TEG) power output compared to other TE geometries, it also increases the PV temperature the most, therefore the overall PV-TE performance using such geometry is reduced. Consequently, asymmetrical TEG (case 4) is recommended for TEG only system while symmetrical TEG (case 1) is recommended for hybrid PV-TE under transient conditions. In addition, shorter thermoelectric legs provide enhanced performance.

Keywords: Photovoltaic-thermoelectric; Asymmetrical legs; Transient study; Finite element method

1. INTRODUCTION

Conventional energy sources are limited in supply and they cause serious environmental issues which affect the climate and health of people. Solar energy is a clean and renewable energy source which can satisfy the global energy demand [1]. The two most common ways to utilize solar energy is to convert it into easily harnessed forms: electrical and thermal energy [2]. Photovoltaic (PV) can convert solar radiations into electricity directly however its conversion efficiency is low due to increased temperature. A thermoelectric generator (TEG) is a waste heat recovery device which operates on the principle of Seebeck effect to generate electricity from waste heat [3]. Therefore, combining a photovoltaic with a thermoelectric generator can potentially provide an improved performance.

Hybrid photovoltaic-thermoelectric (PV-TE) systems can be integrated using either the direct coupling or spectrum splitting approach. Direct coupling requires the thermoelectric generator to be attached directly behind the photovoltaic [4] while spectrum splitting requires the use of a beam splitter [5]. Optimizing the geometry of a thermoelectric generator is an effective method to enhance its performance [6]. Shittu et al. [7] presented a parametric study on the optimum thermoelectric geometry in a hybrid PV-TE uni-couple under steady state conditions and found that the optimum geometry of TEG in a hybrid system varies with solar cell used. Similarly, Li et al. [8] argued that the optimum TE geometry in a hybrid PV-TE is different from that of the TE only. Kossyvakis et al. [9] performance an experimental and numerical study on the performance of a hybrid PV-TE and found that short thermoelectric leg is better for hybrid system performance enhancement.

This paper presents a three-dimensional numerical investigation of a hybrid PV-TE under varying weather conditions using COMSOL Multiphysics software. A comparison of the effect of four different TE geometry on the efficiency and power output of PV-TE under transient conditions is presented and the effect of thermoelectric leg height is investigated.

2. MODEL DESCRIPTION

2.1 Physical model

The schematic diagrams of the four different thermoelectric (TE) geometries considered in this hybrid PV-TE study are shown in Fig. 1. The conventional symmetrical TE geometry is considered as Case 1 (Fig. 1a), while the combined symmetrical and asymmetrical geometry is considered as Case 2 and Case 3 depending on which leg is made asymmetrical. In Case 2 (Fig. 1b), only the N-type leg is made asymmetrical while in Case 3 (Fig. 1c), only the P-type leg is made asymmetrical. In addition, the asymmetrical TE geometry is considered as Case 4 (Fig. 1d). In this study, a PV-TE uni-couple is considered to save computation time and for detailed parametric study. The geometrical properties of the hybrid system components are listed in Table 1.

Table 1. Geometrical properties.

Parameter	Value
PV	
Area	4.5mm x 2.5mm
Glass thickness	3mm
EVA thickness	0.38mm
Silicon thickness	0.3mm
Tedlar	0.17mm
TEG	
Area	4.5mm x 2.5mm
Leg area	1.5mm x 1.5mm
Leg height	1mm
Copper thickness	0.3mm
Ceramic thickness	0.8mm

The asymmetrical leg is achieved by making the width of the hot side half of that of the cold side. All layers of the PV are of equal dimensions and the TEG covers the back of the PV entirely. The other simulation parameters used for modelling the PV are obtained from [10] while those used for modelling the TEG are obtained from [11]. The weather data used for the transient study is obtained from [10] for a city of Shiraz in Iran. Temperature dependent Bismuth telluride (Bi_2Te_3) are used while the radiative and convective heat losses are considered on the top surface (glass) of the PV and the ambient temperature is assumed as the initial temperature of the system. The TEG is connected to an external load resistance and impedance matching is done to obtain maximum power output. Finally, a constant temperature boundary condition of 293.15K is assumed on the TEG cold side and a concentration ratio value of 10 is used in all simulations to increase the solar radiation absorption.
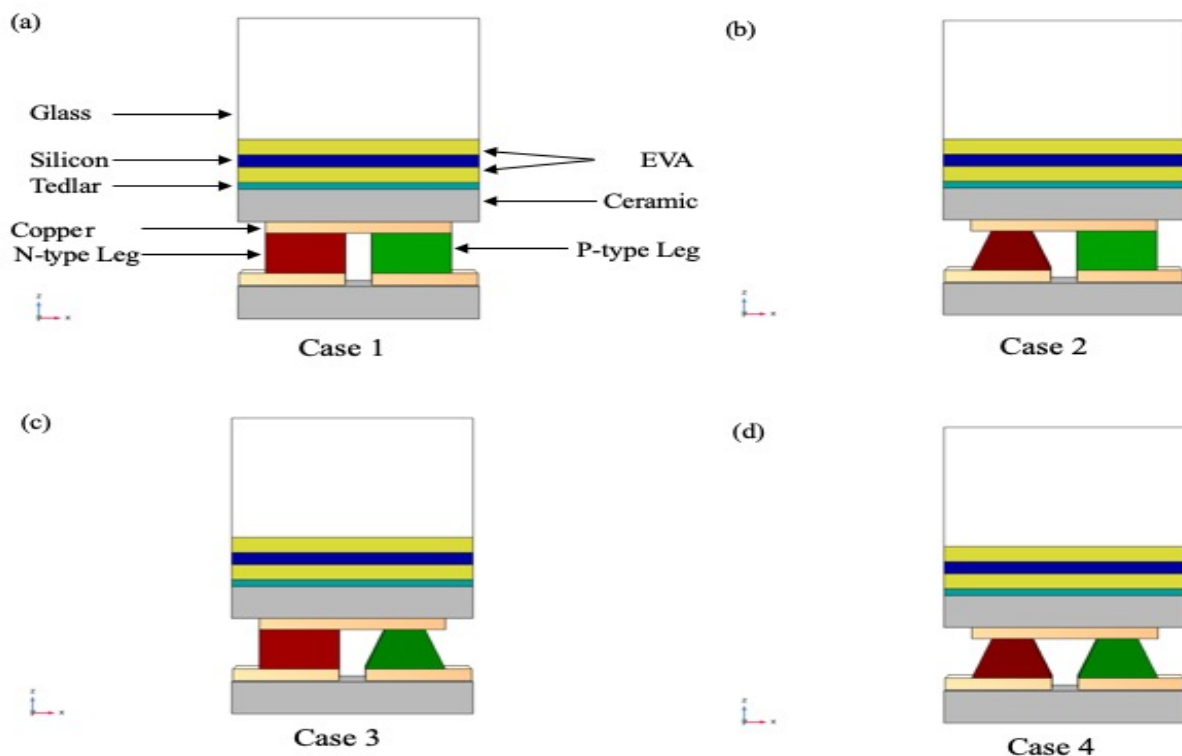

Fig. 1. Schematic diagram of photovoltaic-thermoelectric with different TE geometry.

2.2 Governing equations

The volumetric energy absorption of each layer is given as:

$$\dot{q}_{sol,i} = \frac{G_{rec,i} \times \alpha_i \times A_i \times C}{V_i} \qquad (1)$$

$$G_{rec,i} = G_{rec,i-1} \times [(1 - \alpha_{i-1}) - \rho_{i-1}] \qquad (2)$$

where α_i, ρ_i and V_i are the absorptivity, reflectivity and volume of the ith layer respectively. $G_{rec,i}$ is the solar radiation intensity received at each layer, $\dot{q}_{sol,i}$ is the volumetric heat source at each layer, A_i is the area of the ith layer and C is solar concentration ratio.

In the polycrystalline silicon layer, power generation is considered as an internal heat sink and can be defined as:

$$\eta_{pv} = \eta_{ref}[1 - \beta(T_c - T_{ref})] \qquad (3)$$

$$\dot{P}_{gen} = \dot{q}_{sol,si} \times \eta_{pv} \qquad (4)$$

where η_{ref} is the reference efficiency (15.6%) of the polycrystalline silicon solar cell and β is the temperature coefficient (0.0045/K). T_c is the average temperature of the silicon layer, T_{ref} is the reference temperature of 298.15K and η_{pv} is the efficiency of the PV.

The electrical performance of the TEG is expressed as [3]:

$$V_{OC} = \alpha \Delta T \qquad (5)$$

where V_{OC} is the open circuit voltage, α is the Seebeck coefficient and ΔT is the TEG temperature difference.

$$V_L = V_{OC} - R_{in}I = R_L I \qquad (6)$$

Where V_L is the output load voltage, R_{in} is the internal resistance of the TEG and I is the TEG current. The output power of the TEG (P_{teg}) is given as,

$$P_{teg} = V_L I = R_L I^2 \qquad (7)$$

$$\eta_{teg} = P_{teg} \times Q_h \qquad (8)$$

$$P_{pv-te} = \dot{P}_{gen} + P_{teg} \qquad (9)$$

$$\eta_{pv-te} = \eta_{pv} + \eta_{teg} \qquad (10)$$

where η_{teg} is the TEG efficiency, Q_h is the input heat flux at the top surface of the TEG, P_{pv-te} is the PV-TE power output and η_{pv-te} is the PV-TE efficiency.

2.3 Computational method

COMSOL Multiphysics software which is based on finite element method is used for this numerical study. Four different mesh settings (coarser, coarse, normal and fine) are tested based on COMSOL's in built mesh settings and the little discrepancies between the results shown in Table 2 proves that the mesh converges therefore, Fine mesh is used throughout this study for increased accuracy. In addition, the numerical model used in this study has been validated and used in a recently published paper by the authors [11].

Table 2. Mesh convergence test.

Total number of elements	Element size	Average cell temperature (K)	Total power output (W)
3,005	Coarser	310.29	0.00836
4,817	Coarse	310.28	0.00836
8,612	Normal	310.23	0.00835
12,447	Fine	310.23	0.00835

3. RESULTS AND DISCUSSION

3.1 Effect of thermoelectric geometry

The effect of TE geometry on the transient performance of the hybrid PV-TE is shown in Fig. 2 for the four different cases considered. Fig. 2a shows that the overall efficiency and power output of the PV-TE uni-couple for the four geometries (Case 1-4) considered are similar. However, the performance of the hybrid system using the symmetrical geometry (Case 1) is slightly better. The superiority of the Case 1 geometry for the PV-TE will be more pronounced when a full TEG with thermoelectric couples are used. Fig. 2b shows that the Case 1 geometry provides the best PV efficiency and power output compared to the other geometries. In addition, it is clear that the asymmetrical geometry (Case 4) reduces the performance of the PV. However, the asymmetrical geometry is best suited for the TEG as shown in Fig 2c. The superiority of the Case 4 geometry in providing enhanced TEG efficiency and power output compared to other geometries is shown clearly in Fig. 1c. Therefore, asymmetrical thermoelectric legs (Case 4) are recommended for TEG only applications.
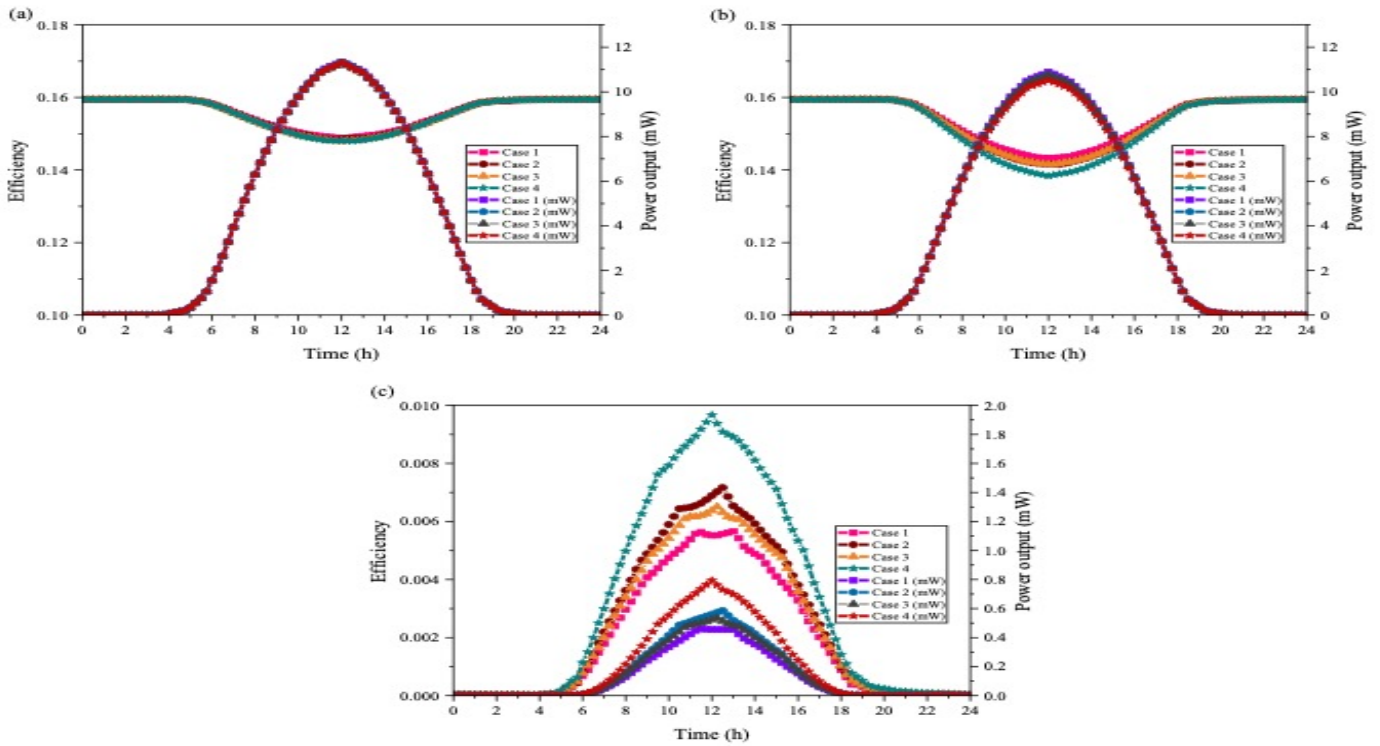
3

Fig. 2. Efficiency and power output of (a) hybrid PV-TE uni-couple (b) PV in PV-TE and (c) TE in PV-TE.

3.2 Effect of geometry on temperature distribution

The average temperature of the polycrystalline silicon layer in the PV-TE for the different geometries considered and the corresponding TEG temperature difference is shown in Fig 3a. As seen, Case 4 provides the highest PV temperature thereby leading to a decreased efficiency. However, Fig. 3a also shows that Case 4 provides the highest TEG temperature difference thereby providing increased TEG efficiency and power output. The temperature distribution of the hybrid PV-TE uni-couple for Case 1 at 12 noon is shown in Fig. 3b. As seen, the PV layer has the highest temperature while the TEG cold side has the lowest temperature due to the fixed temperature boundary.
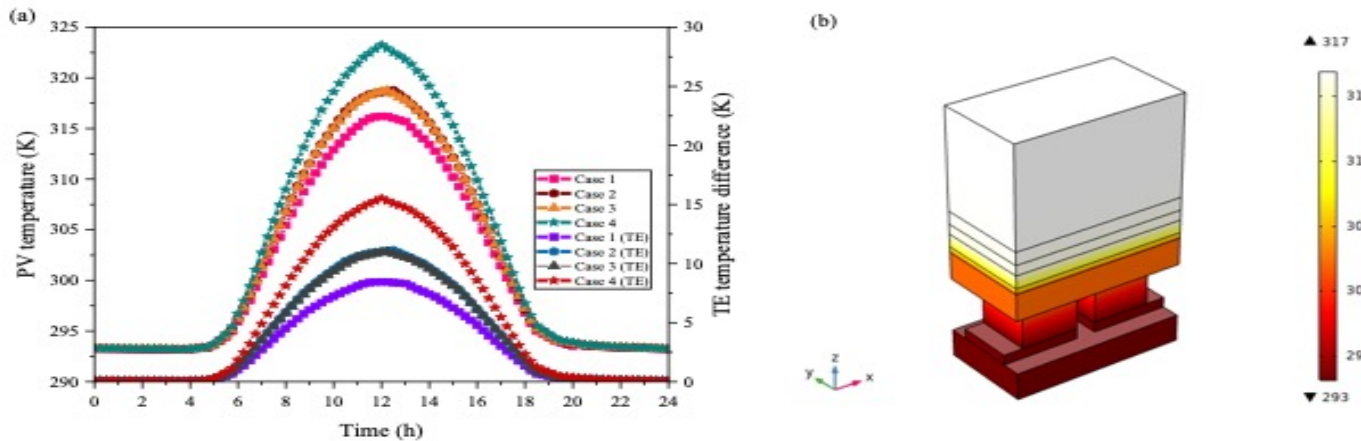

Fig 3. Temperature distribution in (a) PV layer and TEG (b) PV-TE uni-couple.

3.3 Effect of thermoelectric leg height

The TE leg height is an important parameter that influences the performance of the hybrid PV-TE. Fig. 4a shows the PV-TE power output variation with the leg height and it can be seen clearly that Case 1 provides the best power output compared to other geometries.

In addition, it can be seen that the decrease in power output in Case 1 is less rapid compared to the other cases. Furthermore, it can be seen from Fig. 4a and Fig. 4b that the power output decreases as the leg height increases. However, the power output of the TE in PV-TE increases as the leg height increases due to the increase in PV temperature which leads to an increased TEG temperature difference.
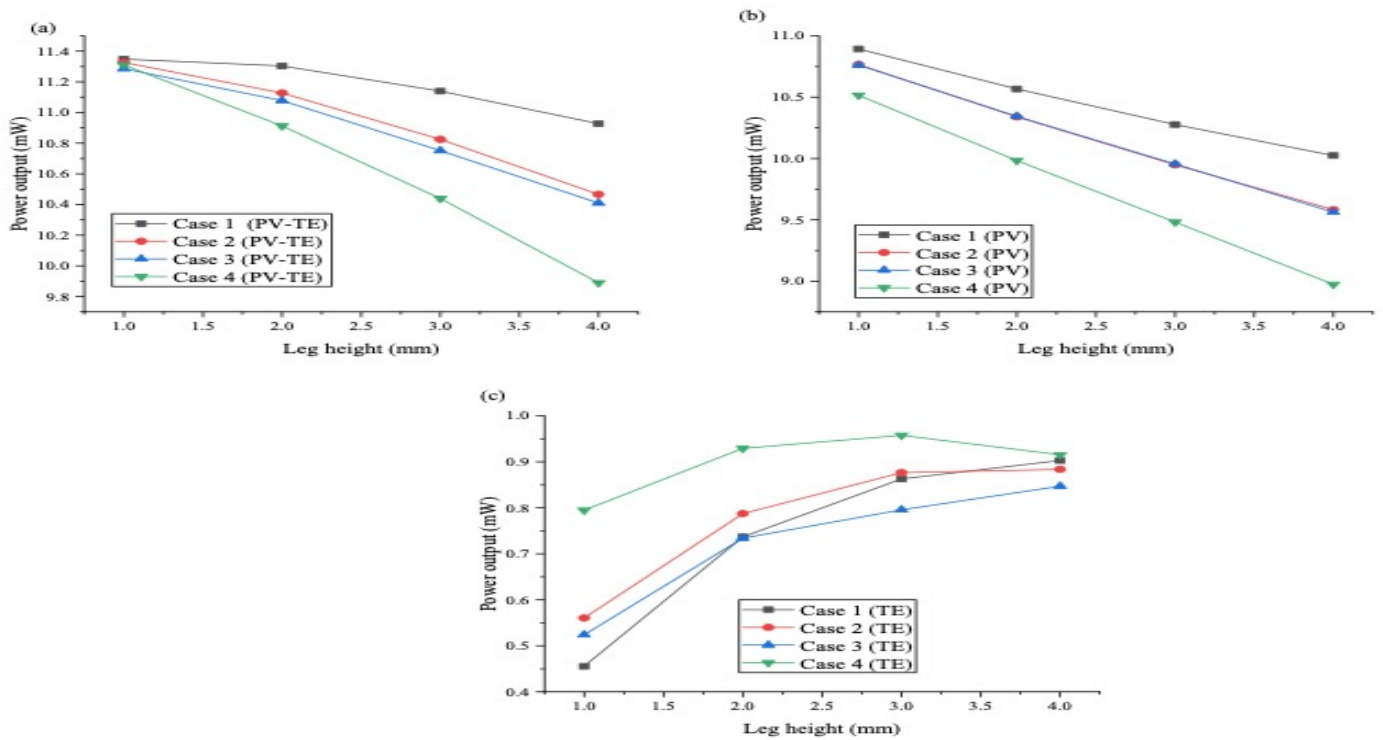
4

Fig. 4. TE leg height variation with power output in (a) PV-TE (b) PV in PV-TE and (c) TE in PV-TE.

4. CONCLUSION

This study presented a parametric and numerical investigation of a hybrid PV-TE uni-couple under varying weather conditions. Three-dimensional finite element simulation software, COMSOL Multiphysics is used for the numerical study and temperature dependent Bismuth telluride (Bi_2Te_3) is considered. The effect of thermoelectric geometry and leg height on the transient performance of the PV-TE is studied and results show that the conventional symmetrical TEG (Case 1) is beneficial for PV-TE while the asymmetrical TEG (Case 4) is beneficial for TEG only under varying weather conditions. Furthermore, shorter thermoelectric legs are recommended for performance enhancement.

REFERENCE

[1] Shittu S, Li G, Akhlaghi YG, Ma X, Zhao X, Ayodele E. Advancements in thermoelectric generators for enhanced hybrid photovoltaic system performance. Renew Sustain Energy Rev 2019;109:24–54.

[2] Li G, Shittu S, Diallo TMO, Yu M, Zhao X, Ji J. A review of solar photovoltaic-thermoelectric hybrid system for electricity generation. Energy 2018;158:41–58.

[3] Shittu S, Li G, Zhao X, Ma X, Akhlaghi YG, Ayodele E. High performance and thermal stress analysis of a segmented annular thermoelectric generator. Energy Convers Manag 2019;184:180–93.

[4] Fisac M, Villasevil FX, López AM. High-efficiency photovoltaic technology including thermoelectric generation. J Power Sources 2014;252:264–9.

[5] Elsarrag E, Pernau H, Heuer J, Roshan N, Alhorr Y, Bartholomé K. Spectrum splitting for efficient utilization of solar radiation: a novel photovoltaic–thermoelectric power generation system. Renewables Wind Water, Sol 2015;2:16.

[6] Shittu S, Li G, Zhao X, Ma X, Akhlaghi YG, Ayodele E. Optimized high performance thermoelectric generator with combined segmented and asymmetrical legs under pulsed heat input power. J Power Sources 2019;428:53–66.

[7] Shittu S, Li G, Zhao X, Ma X. Series of detail comparison and optimization of thermoelectric element geometry considering the PV effect.

Renew Energy 2019;130:930–42.

[8]   Li G, Shittu S, Ma X, Zhao X. Comparative analysis of thermoelectric elements optimum geometry between Photovoltaic-thermoelectric and solar thermoelectric. Energy 2019;171:599–610.

[9]   Kossyvakis DN, Voutsinas GD, Hristoforou E V. Experimental analysis and performance evaluation of a tandem photovoltaic-thermoelectric hybrid system. Energy Convers Manag 2016;117:490–500.

[10]   Motiei P, Yaghoubi M, GoshtashbiRad E, Vadiee A. Two-dimensional unsteady state performance analysis of a hybrid photovoltaic-thermoelectric generator. Renew Energy 2018;119:551–65.

[11]   Shittu S, Li G, Zhao X, Akhlaghi YG, Ma X, Yu M. Comparative study of a concentrated photovoltaic-thermoelectric system with and without flat plate heat pipe. Energy Convers Manag 2019;193:1–14.